Analyst

Accepted Manuscript

This article can be cited before page numbers have been issued, to do this please use: B. Tengan, J. AGONGO, M. ARMBRUSTER, C. Arnatt and J. Edwards, *Analyst*, 2026, DOI: 10.1039/D6AN00437G.

ROYAL SOCIETY OF CHEMISTRY

rsc.li/analyst

View Article Online
DOI: 10.1039/D6AN00437G

Barcoding for Isobaric Tagging of Carboxylic Acids and Amines Metabolites

Briana M. Tengan, Michael R. Armbruster, Julius Agongo, Christopher K. Arnatt, and James L. Edwards

Department of Chemistry and Biochemistry, Saint Louis University, Saint Louis, Missouri

Abstract

Conventional isobaric platforms in metabolomic analyses are designed to label a single functional group, typically primary amines. This specificity restricts the range of detectable analytes in a single injection, limiting overall chemical coverage of metabolites, and potentially reducing the depth of biological insight. Using a proof-of-concept 2-plex isobaric barcode tagging scheme, amine-containing metabolites are selectively labeled using acid barcode tags. Acid-containing metabolites (carboxylate) are derivatized using amine barcode tags. This allows for broad coverage of two metabolite classes in a single injection in a 30-minute LC gradient. These barcode tags undergo double fragmentation to generate cyclized products and distinct reporter ions that are specific to each metabolite class, enabling accurate quantitation. This tagging scheme also serves as an untargeted approach for identifying metabolites not present in the user's metabolic library. Tagged acid and tagged amine analytes are mixed at ratios of 1:2:5:10 using various amounts of *Escherichia coli* lysate to produce a 10-fold linear dynamic range, an average linearity (R^2) of 0.99, and an average RSD of 2.64%. Metabolic changes in amine and carboxylic acid metabolism of genetic knockout PanC and wild-type *Escherichia coli* were characterized using this method.

1. INTRODUCTION

Accurate LC-MS based quantitative metabolomics is hindered by low throughput, variable matrix effects, instrument signal drift, and retention time shifts. Approaches to mitigate these difficulties often lead to prolonged analysis times.[1, 2] Chemical isotope labeling (CIL) is[2] designed to 1) increase ionization efficiency which enhances signal response[3] and 2) improve quantitation through isotope ratio mass spectrometry. These tags render a mass difference for the same analyte from various samples. which enables multiplexing and accounts for matrix effect, as well as signal and chromatographic shifts.[2, 4]

CIL presents challenges to metabolite coverage.[5, 6] For mass shift isotope labeling, the number of analyte peaks increases proportionally to the number of isotope tags used. As the level of multiplexing increases, the spectral complexity in the full MS increases. This requires substantial

View Article Online
DOI: 10.1039/D6AN00437G

chromatographic resolution to avoid overlapping MS signal from different analytes.[4] CIL typically reacts with one class of moieties for analysis, which inherently limits metabolite coverage.

Isobaric tagging is used to alleviate spectral complexity in full MS.[7] Isobaric tags have the same nominal mass but generate distinct reporter ions during MS/MS, allowing differentiation and quantification of analytes.[8] Isobaric tags are designed to include 1) a reactive moiety that targets a specific functional group for labeling; 2) a balancer group isotopically labeled to ensure the same mass of overall tag; and 3) a reporter group that incorporates unique isotopes enabling relative quantification across different samples.[4, 9 10 11 12 7]. Although isobaric tagging offers throughput and quantitative advantages, their analytical performance can be confounded by isobaric ratio compression. This phenomenon is typically driven by the co-isolation and co-fragmentation of interfering ions, which distorts reporter ion intensities and therefore true abundance differences.

Neutral loss-based isobaric tags can be used to remedy chimeric spectra and reporter ion distortion associated with conventional isobaric tags (e.g., TMT,[9] iTRAQ,[10] DiART,[11] DiLeu[12]) that often rely on a1-type fragmentation.[7] However, interfering ions may exhibit compression and distortion even with neutral-loss isobaric tags. Previous work on neutral-loss isobaric tags shows that the reporter group remains attached to the analyte. This imparts a distinct mass shift in the MS/MS scan that distinguishes co-isolated precursors .[7, 13] A quaternary amine neutral loss isobaric tag has been reported for the quantitation of acid metabolites.[2] The neutral loss of the trimethylamine produced a cyclized reporter ion, which remains attached to the analyte. Advances in this tag have generated a set of dual-fragmentation, neutral-loss isobaric reagents for the quantitation of thiols.[7]

A major limitation of using conventional isobaric platforms in metabolomics is their tagging a single functional group, typically primary amines.[9 10 11 12 7] This specificity restricts the range of detectable analytes in a single injection which limits overall chemical coverage and potentially reducing the depth of biological insight. In this current work, we expand metabolite coverage to analyze 100 targeted amines and carboxylates using a proof-of-concept 2-plex isobaric barcode tagging scheme in a single injection. The barcoding strategy uses moiety-specific chemical tags that serve as identifiers for different classes of metabolites.

Barcode tags are designed to selectively label either amine-containing or acid-containing (carboxylate) metabolites, which generate distinct reporter ions upon fragmentation that are exclusive for each class of metabolite, as presented in Figure 1. The labeling of carboxylate analyte using a D_3-neucode pyruvate and a D_0-neucode pyruvate-D_3 amine tags is shown in

View Article Online
DOI: 10.1039/D6AN00437G

Figure 1 A1. D_0-neucode alpha-ketoisocaproic-D_3 and D_3-neucode alpha-ketoisocaproic acid tags are used for the tagging of amine analytes, as illustrated in Figure 1 B1. When a higher-energy collisional dissociation (HCD) is applied, it causes the tagged analyte to undergo double fragmentation to produce a cyclized product and reporter ions[7], as shown in Figure 1 A2 and B2. Specifically, amine barcodes produce reporter ions at m/z 84.0814 and 87.1002 (Figure 1 A3), while acid barcodes yield reporter ions at m/z 126.1276 and 129.1465 (Figure 1 B3). These reporter ions serve as identifiers, enabling the identification and accurate quantification of metabolite classes in complex mixtures. This barcoding framework is inherently scalable and could be expanded to high-level multiplexing, enabling high-throughput quantification of metabolites across large sample sets while maintaining class specificity.

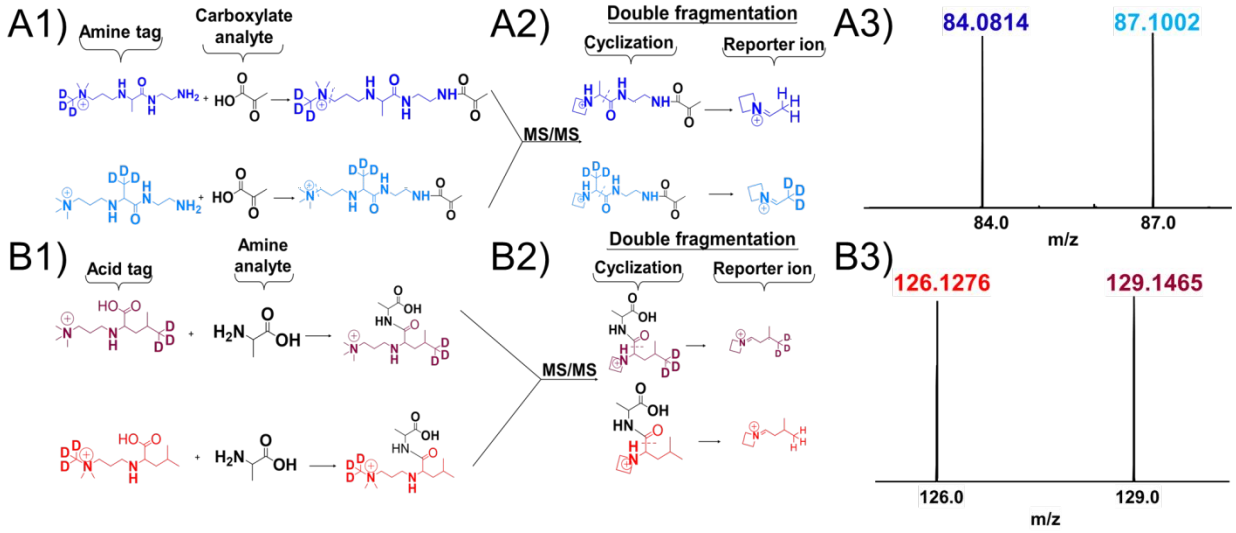

Figure 1. Double fragmentation of (A1) a derivatized carboxylate metabolite using two variants of amine barcode tag and (B1) derivatization of an amine metabolite using two variants of amine barcode tag. The labeled metabolites undergo double fragmentation upon HCD activation (A2 and B2). The first step of fragmentation involves cyclization following trimethylamine neutral loss. Tags undergo a second fragmentation to generate distinct reporter ions at m/z 84.0814 and 87.1002 (A3) for acid metabolites, and at m/z 126.1276 and 129.1465 (B3) for amine metabolites.

2. METHODS

2.1 Reagent and Standard Stock

All acid and amine-containing metabolite standards, 4-(4,6-dimethoxy-1,3,5-triazin-2-yl)-4- 4-methylamorpholinium chloride (DMTMM) and N-methylmorpholine (NMM), Hexafluorophosphate azebenzotriazole tetramethyl uronium (HATU), hydroxybenzotriazole (HOBT), *N*,*N*-Diisopropylethylamine (DIPEA), and pyridine were purchased from MilliporeSigma (St. Louis, MO,

View Article Online
DOI: 10.1039/D6AN00437G

USA). Ammonium acetate, acetic acid, acetonitrile (ACN), and LC-MS grade water were obtained from Fisher Scientific (Pittsburgh, PA USA). Each metabolite stock was prepared at 100μM for each standard, and a final concentration of 5μM mixed acid and 5μM mixed amine-containing metabolites in 80% ACN:20%H_2O was generated. 3-(dimethylamino)-1-propylamine, iodomethane, pyruvate, and alpha-ketoisocaproic acid were purchased from MilliporeSigma (St. Louis, MO USA). Pyruvate-D_3, alpha-ketoisocaproic-D_3, and methyl iodide-D_3 were obtained from Cambridge Isotope Laboratories (Boston, MA, USA). Two *Escherichia coli (E. coli)* strains: Wild-type (BW 25113, i.e. wt) and PanC gene mutant (JW 0129, i.e. PanC KO) were purchased from Horizon Discovery (Lafayette, CO, USA). The WT and PanC KO (ΔpanC750::kan) used in this study were derived from the Keio collection in the *E. coli BW25113* genetic background and contain a kanamycin-resistance cassette.

M9-media was prepared according to previous reports using the following: potassium phosphate monobasic (KH_2PO_4), sodium phosphate dibasic anhydrous (Na_2HPO_4), ammonium chloride (NH_4Cl), sodium chloride (NaCl), magnesium sulfate heptahydrate ($MgSO_4.7H_2O$), and calcium chloride dihydrate ($CaCl_2.2H_2O$) were purchased from Fisher Scientific (Pittsburgh, PA, USA). D-glucose was obtained from Millipore Sigma (St. Louis, MO, USA). The M9-salts constituted 3.6g Na_2HPO_4, 3g KH_2PO_4, 1g NH_4Cl, 0.5g NaCl, 491.5mg $MgSO_4.7H_2O$, 14.6 mg $CaCl_2.2H_2O$, 500mg D-glucose.[14]

2.2 Tag Synthesis

2.2.1 D_0-neucode alpha-ketoisocaproic-D_3 and D_3-neucode alpha-ketoisocaproic acid tags synthesis

3-(dimethylamino)-1-propylamine (Scheme 1A) was Boc-protected in 10mL ethanol (EtOH) using a microwave for 10 minutes, as shown in Scheme 1B. The tag was preconcentrated using a rotary evaporator, followed by extraction with 50:50 dichloromethane (DCM)/water. The DCM layer was further washed with water (3X) and preconcentrated to obtain tert-butyl (3-(dimethylamino)propyl) carbamate as the intermediate. The Boc-protected intermediate was selectively methylated using excess Iodomethane in 20 mL of tetrahydrofuran (THF) for 30 minutes, yielding the corresponding mono methylated solid product[2] (Scheme 1B). The tag was washed with THF and filtered under vacuum. The tag was deprotected in 10mL of 4 M Hydrochloric acid (HCl) for 2 hours to form a solid product, which was then filtered and washed with THF. Using 2 equiv of sodium cyanoborohydride and 3 equiv of Sodium bicarbonate ($NaHCO_3$), the tag was functionalized with 1 equiv. of alpha-Ketoisocaproic-d_3 acid by reductive

View Article Online
DOI: 10.1039/D6AN00437G

amination in 20mL of methanol (MeOH) for 2 hours (Scheme 1C). The tag was purified by reverse-phase chromatography and characterized using high-resolution mass spectrometry (Figure S1) and nuclear magnetic resonance (Figure S2). Following the same synthesis scheme, the D_3-neucode alpha-ketoisocaproic acid tag was synthesized using iodomethane-D_3 and alpha-ketoisocaproic acid. The exact masses of D_0-neucode alpha-ketoisocaproic-d_3 and D_3-neucode alpha-ketoisocaproic acid tags are 234.2256. The observed m/z values of the reporter ions are 129.1466 and 126.1278, respectively, as shown in Figure 1 B3.

2.2.2 D_0-neucode pyruvate-D_3 and D_3-neucode pyruvate amine tag synthesis

This synthesis used a reaction scheme similar to the one outlined above, incorporating additional steps. Briefly, 3-(dimethylamino)-1-propylamine (Scheme 1A) is Boc-protected (Scheme 1B), methylated, deprotected, filtered and washed with THF. Using 2 equiv of sodium cyanoborohydride and 3 equiv. of $NaHCO_3$, the tag was functionalized with 1 equiv. of pyruvate-D_3 by reductive amination in MeOH for 2 hours (Scheme 1C). The tag was purified by reverse-phase chromatography. Using 1.5 equiv of DIPEA and 2 equiv of HATU/HOBT, the tag was functionalized with 1.5 equiv of Boc amine by amide coupling in 20mL of dimethyl formamide (DMF), and the reaction was allowed to proceed overnight (Scheme 1D). The tag was purified using an acid-base wash, then dissolved in THF, and deprotected using 5mL of 1 M HCl for 10 min (Scheme 1D). The tag precipitated upon HCl administration and was subsequently rinsed with THF. The tag was then characterized using high-resolution mass spectrometry (Figures S3) and nuclear magnetic resonance techniques (Figures S4). Using a similar synthesis scheme, the D_3-neucode pyruvate tag was synthesized using iodomethane-d_3 and pyruvate. The % yield of all the tags was above 94%. The exact masses of D_0-neucode pyruvate-D_3 and D_3-neucode pyruvate amine tags are 234.2368. The observed m/z values of the reporter ions are 87.0997 and 84.0808 as illustrated in Figure 1 A3.

Scheme 1. Synthetic Routes for Each of the 4 barcode Tags[a]

View Article Online
DOI: 10.1039/D6AN00437G

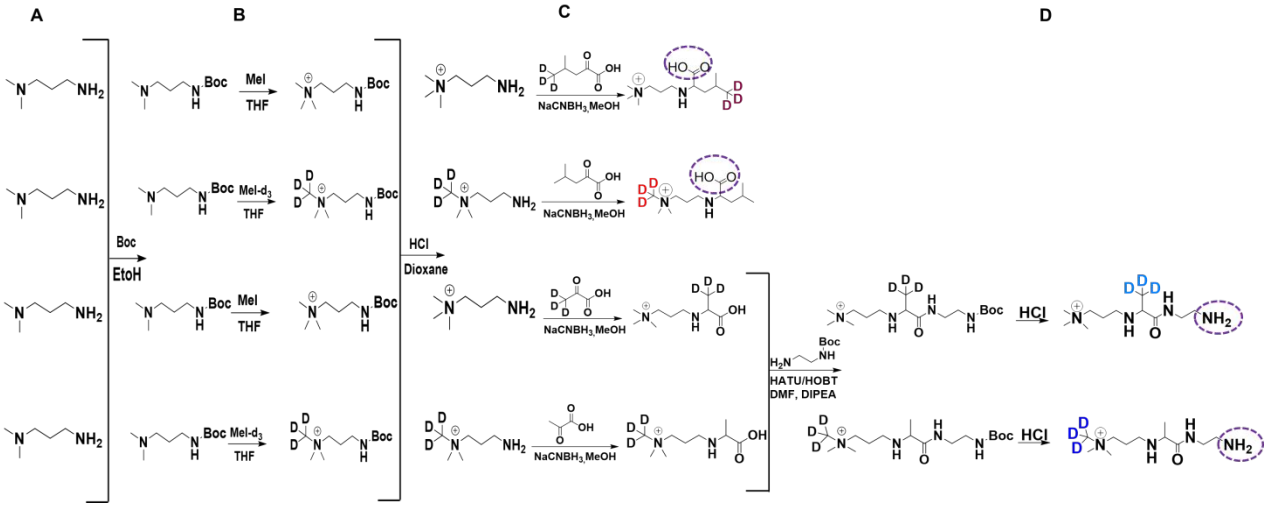

Scheme 1 [a] 3-(Dimethylamino)-1-propylamine, as a starting material, was purchased (**A**). Protection of starting material using Di-*tert*-butyl decarbonate, then methylated using either Iodomethane or Iodomethane-d_3 (**B**). Boc deprotection and tag functionalization (**C**). Boc amine functionalization to tag and Boc deprotection (**D**).

2.3 Cell Culture: Two strains of *E. coli* were pre-cultured in LB broth at 37°C and 250rpm in a shaker overnight. New cultures of WT and PanC KO using LB broth were carried out using a 1:10 serial dilution from pre-cultured WT and PanC KO *E. coli* with optical densities measured at hourly intervals (Figure S10). Once an optical density of 0.6 was achieved for both *E. coli* strains, the cells were centrifuged at 6300rpm at 4 °C for 15 minutes and lysed using a 2:2:1 ratio of methanol, acetonitrile, and water as the lysing solvent. Briefly, the cells were frozen in liquid nitrogen for 2 minutes and then sonicated for 15 minutes. This was done in three separate cycles and stored at -20°C for one hour to enhance metabolite extraction. Afterward, the cells were centrifuged, and the supernatant was collected and stored at -80°C for further analysis. The *E. coli* strains were cultured and lysed in parallel to mitigate sample preparation bias.

To determine the growth conditions of WT and PanC KO in M9 salts, the two *E. coli* strains were pre-cultured in LB broth for 6 hours in a shaker at 37°C and 250rpm. Cells were centrifuged to remove supernatant. Cell pellets were resuspended and new cultures were carried out using a 1:10 serial dilution of the precultured *E. coli* strains in 750 mL of M9-glucose salts, placed in a shaker at 37°C and 250rpm for 24 hours.

2.4 Tagging Scheme

2.4.1 Amine Derivatization

A 500 µL stock solution of 5 µM containing 30 amine metabolite standards was derivatized. For *E. coli* lysate, 30 µL of 50mM D_0-neucode alpha-ketoisocaproic-d_3 and D_3-neucode alpha-

View Article Online
DOI: 10.1039/D6AN00437G

ketoisocaproic acid tags were activated separately using 50µL of 75mM HATU and 100mM HOBT in DMF and 24% pyridine for an hour at room temperature. 40 µL of activated D_0-neucode alpha-ketoisocaproic-d_3 tag was added to 500 µL of WT *E. coli* lysate, and 40 µL of activated D_3-neucode alpha-ketoisocaproic tag was added to 500 µL PanC KO *E. coli* lysate containing 1.5% NMM. The reaction was allowed to proceed for 4 hours at room temperature in a shaker at 25 °C. Following this, the mixture was dried using a vacuum centrifuge, achieving a reaction efficiency of over 95%. Derivatization reaction efficiency was determined using calibration curves generated from untagged metabolites from commercially available standards. Metabolite concentrations were determined in both untagged *E. coli* lysates and tagged lysates. Remaining untagged metabolites from the tagged samples indicated near complete reaction efficiency (>95%). Analysis for the unreacted metabolite is the only way to account for differences in sensitivity of tagged vs untagged metabolites, as there is no commercial standard for the fully tagged counterparts.

2.4.2 Acid Derivatization

70 acid-containing metabolite standards were derivatized at a stock concentration of 5 µM in 500 µL. Into a 500 µL of WT *E. coli* lysate *and* 500 µL PanC KO *E. coli* lysate, 35µL of 25mM of D_0-neucode pyruvate-d_3 and D_3-neucode pyruvate amine tags were added, respectively. 35 µL of 75 mM DMTMM, containing 1.2% NMM, was subsequently added to each Eppendorf tube containing the *E. coli* lysate. The mixture was allowed to react in a shaker at 25°C for 4 hours. Thirty minutes into the reaction, 50 µL of 37 mM DMTMM was added to drive the reaction to > 95% completion. Following this, the mixture was dried using a vacuum centrifuge. All 4 vials of tagged metabolites (acid and amine) were reconstituted in 50µL volume and mixed 1:1.

2.5 LC-MS Analysis

2.5.1 Capillary Liquid Chromatography

A frit was fabricated in a 50-µm inner-diameter capillary column, close to the pulled nano tip. [15, 16] The tip was created using a laser-pulled method.[17] In brief, a window was created in a 27 cm long fused silica capillary by removing the polyimide coating using an electrical arc. A photopolymerized frit was created at the window under a wavelength of 365 nm for 30 min. Nanospray tips were generated using a Sutter CO_2 laser puller model P-2000. The nano-capillary column was then packed with Acquity UPLC Amide 1.7 µm particles using a gas pressure cell. The column length was finally cut to 15 cm. The column was attached to a stainless-steel tee to split the flow.[7] The split was made up of a 50 µm × 75 cm open capillary. A 30-minute gradient method was employed at a controlled flow rate of 0.200 mL/min and an injection volume of 5 µL

View Article Online
DOI: 10.1039/D6AN00437G

(491 nL/min through the capillary column). The mobile phase A comprised 95% acetonitrile (ACN) and 5% water, supplemented with 10 mM ammonium acetate and 0.1% acetic acid. Mobile phase B was 10% ACN and 90% water, which also contained 10 mM ammonium acetate and 0.1% acetic acid.[7] The gradient used for the separation of tagged amines and carboxylates was: 20% B, 0 min; 20% B, 1 min; 95% B, 5 min; 95% B, 22 min; 20% B, 22.1 min**;** 20% B, 30 min.

2.5.2 MS Analysis

Samples were analyzed as previously described using a Q-Exactive orbitrap mass spectrometer (Thermo Fisher Scientific, Waltham, MA) coupled to a Thermo Vanquish LC instrument (Thermo Fisher Scientific, Waltham, MA).[7] All runs were carried out at a spray voltage of 1.75 kV and a capillary temperature of 200 °C.[7] For parallel reaction monitoring (PRM) runs, a maximum Ion injection time of 50ms and an AGC target of $1e^6$, with a resolution of 17.5 K, were used in the MS^1 scan, covering a scan range of 100-600 m/z.[7] In the PRM scan, a 100-inclusion list of analytes with a maximum ion injection time of 100 ms, AGC target of $1e^6$, resolution of 140 K, and an optimal collision energy of 35 were used. Untargeted runs were carried out using a resolution of 70 K, an AGC target of $1e^6$, a maximum Ion injection time of 100ms, and a scan range of 70-800 m/z for the full MS. The data-dependent analysis (DDA)-MS/MS used a 17.5 K resolution, a maximum ion injection time of 50ms, a $2e^5$ AGC target with a DDA setting of 20.0s dynamic exclusion.

2.5.3 Data Extraction and Processing

For targeted metabolomics, the extracted LC-MS data were processed using Xcalibur QualBrowser and Skyline[18]. Known metabolites were quantified using the reporter ion observed by PRM. Data analysis was performed in Excel, and graphs were generated in GraphPad Prism 9. Untargeted metabolites were identified using the R package CluMSID.[19]These samples were analyzed using a DDA method

3 RESULTS AND DISCUSSION

The barcoding scheme for multiplexed analysis uses isobaric tagging to quantify 100 carboxylate and amine metabolites in complex biological mixtures from a single injection. Differential reporter ions of amine and acid tags are generated by using different keto-acid precursors (Figure 2), which, upon fragmentation, indicate the presence of an amine or an acid metabolite. The ability of barcode tags to undergo double fragmentation enables the generation of cyclized products and distinct reporter ions for each metabolite class, thereby reducing the potential for spectral overlap and improving resolution in MS/MS analysis.

View Article Online
DOI: 10.1039/D6AN00437G

The general scheme for our barcode tagging uses two strains of *E. coil* (WT and PanC KO*),* as shown in Figure 2. The barcode acid tags differ from the amine tags in that they use alpha-ketoisocaproic acid (red) and pyruvate (blue) as the central component, respectively (Figure 2A). This yields reporter ions of 126.1276 and 129.1465 m/z for acid tags, and 84.0814 and 87.1002 m/z for amine tags. Each class of tag (acid and amine) uses both isotopic and non-isotopic variants of the keto-acid base, which allows for the two-plex isobaric set to generate distinct reporter ions. The reactive moiety of each tag allows derivatization of amine analytes with acid-tag (red) variants and carboxylate analytes with amine-tag (blue) variants. Because dual fragmentation yields distinct reporter ions, unknown metabolites can be characterized by the presence of appropriate functional groups. These barcode tags are reacted with samples individually and mixed, which increases coverage of the metabolome.

Co-elution of isotopically tagged metabolites is critical to isobaric quantitation. Even small differences in retention times between tags can cause substantial signal variance. Chromatograms show co-elution of tagged metabolites as illustrated in (Figure 2B B1), tagged amine and tagged carboxylate (Figure 2B B1) with near identical peak profiles and retention times. The position of the deuterated methyl group either on the quaternary amine (balancer) or on the keto acid (reporter) of the tags allows for a 2-plex reporter ion in the MS/MS, as presented in Figure 2C.

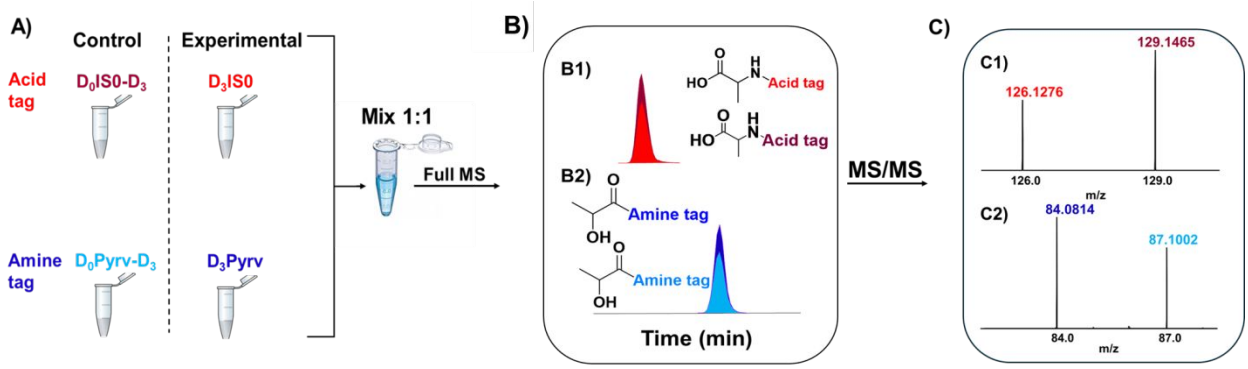

Figure 2: Analytical tagging scheme of amine and acid quantitation. WT and PanC KO *E. coli* were cultured in LB Broth and lysed under the same conditions. (**A**) 500 µL of each WT and PanC KO *E. coli* lysate was derivatized. Two vials of each WT and PanC KO *E. coli* lysate were derivatized with either type of acid or amine tag variant, then mixed at a 1:1 ratio. (**B**) Full MS peaks of tagged (B1) amine and (B2) acid metabolites. (**C**) Each tag undergoes dual fragmentation, first cyclization, following the loss of trimethylamine, then the reporter ion. Triggers of MS/MS fragmentation to generate reporter ions (C1) of m/z 126.1278 and 129.1466 for amine metabolites (C2) 84.0808 and 87.0997 for acid metabolites.

View Article Online
DOI: 10.1039/D6AN00437G

Quantitative parameters for the tags were characterized to ensure appropriate use in biological matrices. The optimal collision energy for the acid and amine tags was evaluated. Tags themselves were analyzed under different collision energies from the HCD cell in triplicate. A nHCD value of 35 was found to produce the most intense reporter ion, as shown in Figure S5. No retention time shifts due to deuterium incorporation around the quaternary amine tags were observed. This resulted in consistent reporter intensity across the top 50% of each peak, as illustrated in Figures S6 and consistent with previous work on reverse-phase columns.[2, 7]

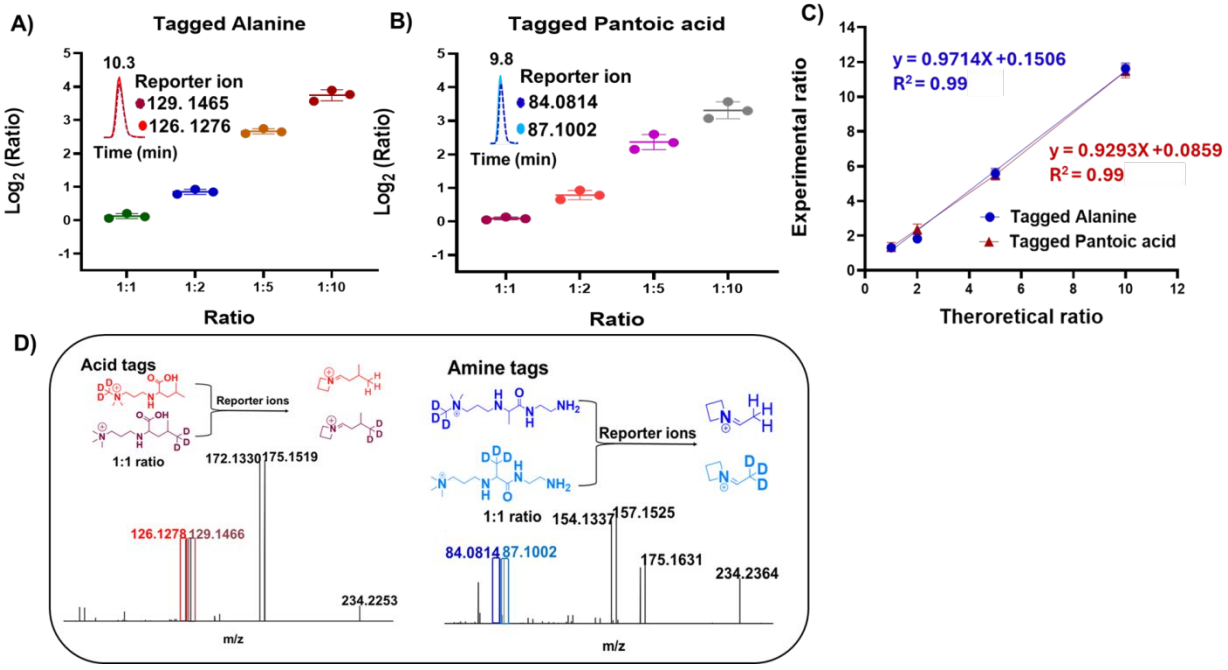

Figure 3. MS/MS reporter ion-based quantification of barcode isobaric tags. **(A & B)** Measured ratios of tagged amine and acid-containing metabolites at mixing ratios of 1:1, 1:2, 1:5, and 1:10. Co-elution of the extracted ion chromatogram of reporter ions of tagged alanine (126.1278 and 129.1466 and pantoic acid (84.0814 and 87.1002) metabolites. **(C)** Linearity and dynamic range of quantification for the experimental to theoretical intensity ratios of amine and acid barcode tags. Each data point represents the mean value of a 1:2:5:10 labeling experiment, with error bars indicating the corresponding standard deviation. **(D)** 1:1 ratio of reporter ions generated from each amine and acid tag variants. Tags undergo dual fragmentation in MS/MS, generating reporter ions of equal intensity for each tag variant.

The analytical performance of this method was evaluated by mixing tagged acid and tagged amine analytes at ratios of 1:2:5:10 using various amounts of *E. coli* lysate. This analytical step used varying volumes of cell lysate and, therefore, cell mass to assess linearity, quantitative accuracy, and to evaluate potential matrix effects in the sample. These data show that the analytical performance is independent of isotopic tag composition. The method had a 10-fold

View Article Online
DOI: 10.1039/D6AN00437G

linear dynamic range for the 100 tagged amine and the tagged acid (Figures 3A and 3B), with an average linearity (R^2) of 0.99 ± 0.027 (Supplemental Table 1). Linearity for tagged alanine was 0.99, while tagged acid pantoic acid showed a linearity of 0.99 (Figure 3). To determine the reproducibility of each tag variant, identical samples were mixed in a 1:1 ratio, yielding an average percentage reaction RSD of 2.64 ± 0.789 (Supplemental Table 1). Overall, these results are consistent with previously reported values in the literature.[2, 7, 20, 21] While both tags contain a tertiary amine to enhance signal intensity, there is a slight difference in sensitivity between them as seen by the slope of their calibration curves with an average tagged amine metabolites 0.9647 ± 0.0116 , and the average tagged carboxylate 0.9349 ± 0.0144 . This may be of interest when exploring larger levels of multiplexing.

The barcode tags were then applied to WT and PanC KO *E. coli* strains to determine if metabolic differences could be uncovered from a genetic knockout. The WT strain was designated as the control sample, and a mutant strain, designated PanC KO, was used as the experimental sample. The PanC KO strain carries a genetic knockout in the pantothenate biosynthesis pathway, specifically affecting the gene encoding pantothenate synthetase (*PanC*)[22] as illustrated in Figure 4A. This enzyme catalyzes the final step in the biosynthesis of pantothenate (vitamin B5), an essential precursor for coenzyme A.

View Article Online
DOI: 10.1039/D6AN00437G

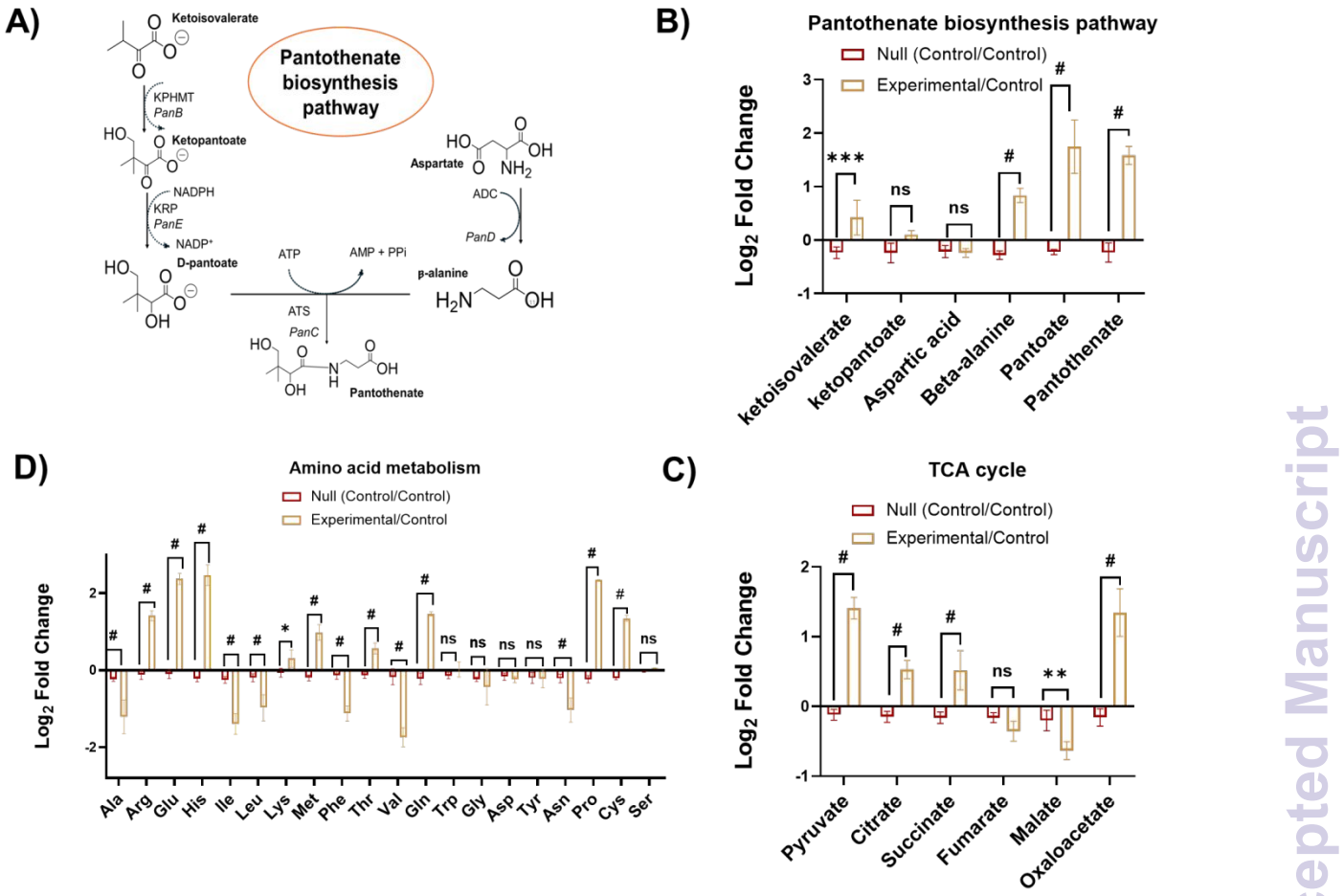

Figure 4. Log_2 fold change of metabolites relative to control compared with a control/control null distribution. Log_2 fold change (Log_2 FC) values for the null distribution were calculated by comparing control samples against other control replicates to estimate baseline variability under no biological change. Experimental Log_2 FC values were calculated relative to the control condition. Bars represent mean values across replicates, and error bars indicate ±SD. The horizontal line at Log_2 FC = 0 denotes 1:1 and no change relative to control. Ns represent no significant difference, * ($p \leq 0.05$), ** ($p \leq 0.01$), *** ($p \leq 0.001$), # (($p \leq 0.0001$).

A total of one hundred known amine- and acid-containing metabolite standards were used to broadly characterize the strains (Table S2). Targeted metabolomic analysis revealed pathway-specific metabolic reprogramming in the PanC KO relative to control (yellow), while the null (control/control, red) comparison remained centered near zero across metabolites, indicating minimal technical or baseline variation. All amino acids, including beta-alanine, were quantified using the acid tag variant. The use of the amine tag for derivatizing the carboxylic group on the amino acids with the DMTMM coupling reagent yields poor reaction efficiency, possibly due to dimerization. The null (control/control, red) represents the derivatized amine and acid-containing

View Article Online
DOI: 10.1039/D6AN00437G

metabolites in WT *E. coli* using D_0 of the tag variants, ratio to the derivatized amine and acid-containing metabolites in WT *E. coli* using D_3 of the tag variants.

Significant increases of metabolites in the pantothenate biosynthesis pathway were observed, particularly pantothenate (Figure 4B). This observation is consistent with prior work showing that PanC KO grown in excess pantothenate elevates intracellular pantothenate and CoA levels through transport/uptake in spite of altered expression.[23] Despite the loss of pantothenate synthetase activity in PanC KO *E. coli,* the cell can import pantothenate from LB Broth via transporters like PanF.[23, 24] LB Broth is composed of yeast extract, and this extract contains pantothenate, enough to aid in the growth of PanC KO *E. coli.*[25-27] When M9 salt was used for PanC KO culture, no growth was observed for 24 hours (data not shown). The seeming discrepancy between PanC KO and the elevation in pantothenate is likely due to importing pantothenate from the media. While not a conclusive part of this study, the lack of growth of PanC KO in M9-glucose minimal media and previous reports support this hypothesis.

To explore the potential impact of elevated pantothenate levels in the PanC KO on CoA enzyme activities, we measured the signal intensities of acetyl-CoA, succinyl-CoA, and malonyl-CoA in both WT and PanC KO strains. Reduced availability of free CoA reduces acetyl-CoA formation, leading to decreased acetyl-CoA levels in the mutant (Figure S7). The findings showed that the PanC KO exhibited increased levels of succinyl-CoA and malonyl-CoA (Figure S7). Given that pantothenate is a precursor in the CoA biosynthetic pathway, the uptake and conversion of extracellular pantothenate from LB Broth suggest an increase in CoA levels[27, 28]. Feedback regulation at pantothenate kinase plays a crucial role in maintaining CoA homeostasis[27]. Consequently, in PanC KO, cells may rely more on external uptake, leading to a distinct rebalancing of intermediate metabolite pools compared to the WT [27].

These regulatory changes have the potential to enhance the flow of carbon into the TCA and fatty acid pathways, leading to accumulation of CoA derivatives such as succinyl-CoA and malonyl-CoA, and increases in various metabolite levels due to downstream reaction and altered CoA utilization.[29, 30] The increased pantothenate levels likely enhanced coenzyme A (CoA) availability, which is consistent with elevated levels of TCA cycle intermediates, including pyruvate, citrate, succinate, and oxaloacetate,[30] while fumarate and malate may be depleted due to their use in biosynthetic processes,[31] as illustrated in Figure 4C.

The CoA availability and altered metabolite abundances lead to enhanced catabolism of branched-chain amino acids such as Val, Leu, and Ile,[32] while the elevated levels of amino acids,

View Article Online
DOI: 10.1039/D6AN00437G

including Glu, Gln, and Arg, support nitrogen balance and anabolic demands[33] [34](Figure 4D). These results are consistent with those reported in the literature, showing that *E. coli* disruptions in pantothenate synthesis can be bypassed through uptake mechanisms or alternative regulatory adaptations that elevate pantothenate and other metabolite levels in the pathway [29, 35, 36].

In the fatty acid and dicarboxylate metabolites (Figure S8A), an increase in fatty acids level such as acetate, caprylate, decanoate, lactate, and hydroxypropionate is consistent with altered fatty acid synthesis associated with perturbed CoA homeostasis.[37] The PanC KO strains are known to exhibit changes in fatty acid–associated metabolites due to CoA's central role in acyl-group activation and fatty acid metabolism, leading to the accumulation of specific organic acids when canonical pathways are constrained.[29, 37-39] Concurrent decreases in dicarboxylates such as propionate, suberate, and glutarate suggest selective depletion of metabolite pools that depend on CoA-linked processing steps.

The results of amino acid derivatives and polyamine-related metabolites profiles (Figure S8B) suggest a compensatory response to PanC KO disruption. Increased levels of cysteine and cystine suggest an enhanced sulfur amino acid availability, which has been linked to stress adaptation and maintaining redox balance, under conditions of perturbed CoA metabolism[40, 41]. Increased ornithine and 1,3-diaminopropane indicate remodeling of polyamine metabolism. Polyamine synthesis is coupled to nitrogen balance and is known to respond to perturbations in central metabolism, such as CoA availability.[42, 43]

The significant increase in hydroxyphenylacetate, hydroxyphenyllactate, pyroglutamate, methyl-oxovalerate, hydroxy, and keto-acid derivatives (Figure S8C) derived from aromatic and branched-chain amino acids is consistent with altered amino acid processing in the PanC KO strain. These metabolites accumulate when amino acid pathways are rebalanced or when downstream reactions requiring CoA are limited, leading to diversion into alternative derivative pools.[44, 45] This pattern has been observed in *E. coli* strains with disruptions in pantothenate or CoA biosynthesis, where amino acid–derived organic acids increase as part of a broader metabolic adjustment.[27, 39]

The results show a significant increase in N-acetylated amino acids in PanC KO (Figure S8D), indicating enhanced amino-acid acetylation. The depletion of acetyl-CoA in the PanC KO strain suggests its usage to enhance amino-acid acetylation.[46] This is consistent with the increased availability of CoA-derived acetyl groups, which are known to support amino acid modification and intracellular homeostasis in *E. coli.* [30, 47]

View Article Online
DOI: 10.1039/D6AN00437G

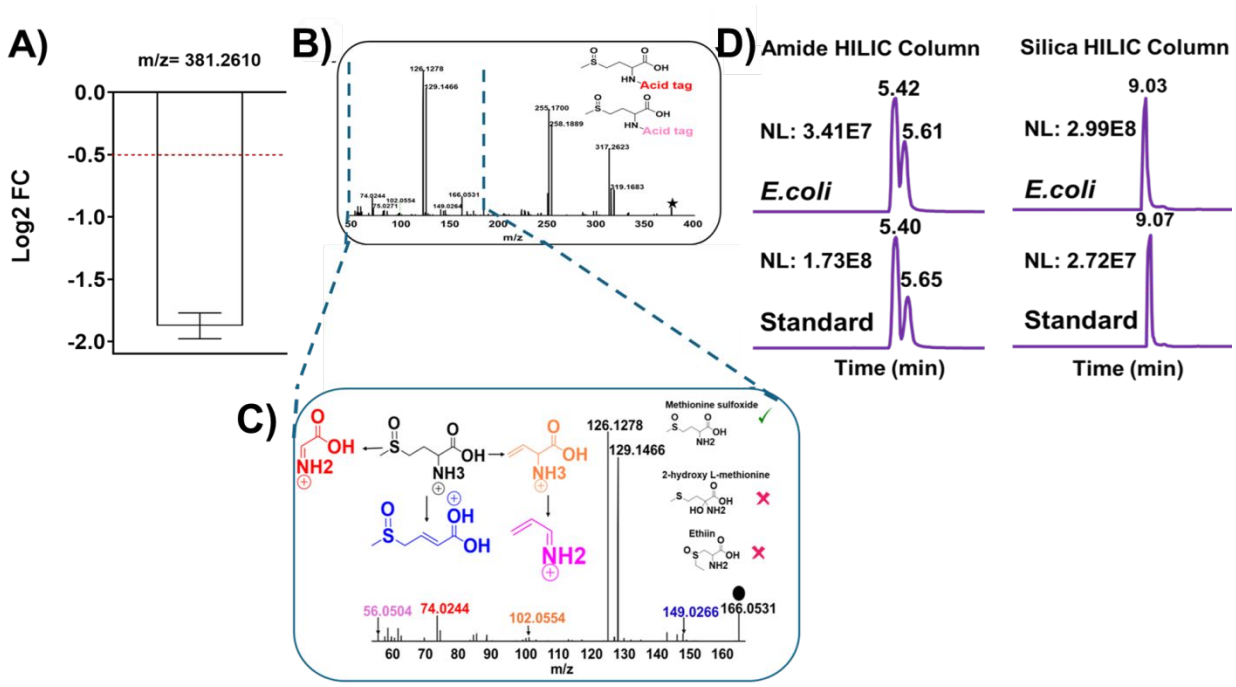

Figure 5. Untargeted barcode isobaric tagging in a separate injection for metabolite quantitation. An untargeted m/z quantified using the R package CluMSID **(A)**. MS/MS spectrum of labeled untargeted mass containing a unique amine reporter ion, indicating that these metabolites have been labeled by an acid barcode tag **(B)**. The black circle over 166.0531 is the m/z of the untagged metabolite. The mass of the tag is subtracted from the untargeted mass, and searching the database yielded three metabolites with the same mass (black circle), and the fragmentation pattern is consistent with methionine sulfoxide **(C)**. Validation of methionine sulfoxide using level one confirmation **(D)**.

Our proof-of-concept barcode tagging scheme not only targets one hundred specific metabolites but also serves as an untargeted approach. Using the DDA method, over 150 masses were quantified, expanding analytical capabilities beyond the initial target list. The identification of these additional untargeted masses is based on the detection of unique reporter ions of the barcode isobaric tags, highlighting the versatility and potential of this tagging scheme. An untargeted m/z of 381.261 (Figure 5A) containing reporter ions of 126.1278 and 129.1466 (Figure 5B) indicates the presence of an amine-containing metabolite. To identify this metabolite, the mass of the acid tag was subtracted from the untargeted mass, resulting in an m/z of 166.0531 (Figure 5C). This value was then cross-referenced with a metabolic database, leading to potential hits as methionine sulfoxide, 2-hydroxy-L-methionine, or ethiin metabolites, all of which share the same mass (Figure 5C).

View Article Online
DOI: 10.1039/D6AN00437G

The fragmentation pattern indicates that the unknown mass is methionine sulfoxide. To explore this further, the barcode acid tag was used to label both the methionine sulfoxide standard and the methionine sulfoxide present in the *E. coli* lysate. Preliminary confirmation at level one shows a consistent retention time and peak shape between the methionine sulfoxide standard and the methionine sulfoxide in the *E. coli* lysate across different amide and silica columns (Figure 5D).

Similarly, gamma-aminobutyric acid, which was not present in the initial 100 metabolite standards, was quantified using an untargeted approach and validated at the one-level confirmation using a chemical standard, as shown in Figure S9B. These examples show the potential for uncovering novel metabolic changes from genetic knockouts as well as identifying new metabolites that are not present in the user's metabolic library.

4. CONCLUSION

A proof-of-concept 2-plex barcode isobaric tags has been developed, enabling wide coverage of metabolites. These tags undergo double fragmentation to produce a cyclized product, followed by a distinct reporter ion that serves as an identifier for acid- and amine-containing metabolites. The acid tags are used for the derivatization of amine-containing metabolites, while the amine tags are used for the tagging of acid-containing metabolites. In the PanC KO experimental strain, significant changes in intracellular metabolite abundances were observed relative to the control, confirming that the changes are specifically associated with PanC KO uptake. This 2-plex barcode isobaric tagging scheme also doubles as an untargeted barcode isobaric tagging platform, enabling metabolite identification and quantitation when standards are unavailable.

This method could be expanded up to 128-plex multiplexing with broad metabolite coverage.

View Article Online
DOI: 10.1039/D6AN00437G

View Article Online
DOI: 10.1039/D6AN00437G

References

(1) Plumb, R. S.; Gethings, L. A.; Rainville, P. D.; Isaac, G.; Trengove, R.; King, A. M.; Wilson, I. D. Advances in high throughput LC/MS based metabolomics: A review. *TrAC Trends in Analytical Chemistry* **2023**, *160*, 116954.
(2) Armbruster, M. R.; Grady, S. F.; Arnatt, C. K.; Edwards, J. L. Isobaric 4-plex tagging for absolute quantitation of biological acids in diabetic urine using capillary LC–MS/MS. *ACS Measurement Science Au* **2022**, *2* (3), 287-295.
(3) Huang, T.; Armbruster, M. R.; Coulton, J. B.; Edwards, J. L. Chemical tagging in mass spectrometry for systems biology. *Analytical chemistry* **2018**, *91* (1), 109-125.
(4) Sivanich, M. K.; Gu, T. J.; Tabang, D. N.; Li, L. Recent advances in isobaric labeling and applications in quantitative proteomics. *Proteomics* **2022**, *22* (19-20), 2100256.
(5) Guo, K.; Li, L. Differential 12C-/13C-isotope dansylation labeling and fast liquid chromatography/mass spectrometry for absolute and relative quantification of the metabolome. *Analytical chemistry* **2009**, *81* (10), 3919-3932.
(6) Zhao, S.; Li, H.; Han, W.; Chan, W.; Li, L. Metabolomic coverage of chemical-group-submetabolome analysis: group classification and four-channel chemical isotope labeling LC-MS. *Analytical Chemistry* **2019**, *91* (18), 12108-12115.
(7) Armbruster, M. R.; Grady, S. F.; Caldwell, R. N.; Arnatt, C. K.; Edwards, J. L. Dual Fragmentation Isobaric Tags for Metabolomics. *Journal of the American Society for Mass Spectrometry* **2023**, *34* (8), 1724-1730.
(8) Frost, D. C.; Greer, T.; Li, L. High-resolution enabled 12-plex DiLeu isobaric tags for quantitative proteomics. *Analytical chemistry* **2015**, *87* (3), 1646-1654.
(9) Thompson, A.; Wölmer, N.; Koncarevic, S.; Selzer, S.; Böhm, G.; Legner, H.; Schmid, P.; Kienle, S.; Penning, P.; Höhle, C. TMTpro: design, synthesis, and initial evaluation of a proline-based isobaric 16-plex tandem mass tag reagent set. *Analytical chemistry* **2019**, *91* (24), 15941-15950.
(10) Wiese, S.; Reidegeld, K. A.; Meyer, H. E.; Warscheid, B. Protein labeling by iTRAQ: a new tool for quantitative mass spectrometry in proteome research. *Proteomics* **2007**, *7* (3), 340-350.
(11) Chong, P. K.; Gan, C. S.; Pham, T. K.; Wright, P. C. Isobaric tags for relative and absolute quantitation (iTRAQ) reproducibility: Implication of multiple injections. *Journal of proteome research* **2006**, *5* (5), 1232-1240.
(12) Frost, D. C.; Feng, Y.; Li, L. 21-plex DiLeu isobaric tags for high-throughput quantitative proteomics. *Analytical chemistry* **2020**, *92* (12), 8228-8234.
(13) Lu, Y.; Zhou, X.; Stemmer, P. M.; Reid, G. E. Sulfonium ion derivatization, isobaric stable isotope labeling and data dependent CID-and ETD-MS/MS for enhanced phosphopeptide quantitation, identification and phosphorylation site characterization. *Journal of The American Society for Mass Spectrometry* **2011**, *23* (4), 577-593.
(14) Soma, Y.; Tominaga, S.; Tokito, K.; Imado, Y.; Naka, K.; Hanai, T.; Takahashi, M.; Izumi, Y.; Bamba, T. Trace impurities in sodium phosphate influences the physiological activity of Escherichia coli in M9 minimal medium. *Scientific reports* **2023**, *13* (1), 17396.
(15) Mostafa, M. E.; Grinias, J. P.; Edwards, J. L. Supercritical fluid chromatography-Nanospray ionization-mass spectrometry (SFC-nSI-MS). *Journal of Chromatography A* **2024**, *1736*, 465377.

View Article Online
DOI: 10.1039/D6AN00437G

(16) Sanders, K. L.; Edwards, J. L. Nano-liquid chromatography-mass spectrometry and recent applications in omics investigations. *Analytical Methods* **2020**, *12* (36), 4404-4417.
(17) Mostafa, M. E.; Grinias, J. P.; Edwards, J. L. Evaluation of nanospray capillary LC-MS performance for metabolomic analysis in complex biological matrices. *Journal of Chromatography A* **2022**, *1670*, 462952.
(18) Sharma, V.; Eckels, J.; Schilling, B.; Ludwig, C.; Jaffe, J. D.; MacCoss, M. J.; MacLean, B. Panorama public: a public repository for quantitative data sets processed in skyline. *Molecular & Cellular Proteomics* **2018**, *17* (6), 1239-1244.
(19) Depke, T.; Franke, R.; Brönstrup, M. CluMSID: an R package for similarity-based clustering of tandem mass spectra to aid feature annotation in metabolomics. *Bioinformatics* **2019**, *35* (17), 3196-3198.
(20) Hao, L.; Zhong, X.; Greer, T.; Ye, H.; Li, L. Relative quantification of amine-containing metabolites using isobaric N, N-dimethyl leucine (DiLeu) reagents via LC-ESI-MS/MS and CE-ESI-MS/MS. *Analyst* **2015**, *140* (2), 467-475.
(21) Tian, X.; de Vries, M. P.; Permentier, H. P.; Bischoff, R. A versatile isobaric tag enables proteome quantification in data-dependent and data-independent acquisition modes. *Analytical Chemistry* **2020**, *92* (24), 16149-16157.
(22) Suresh, A.; Srinivasarao, S.; Khetmalis, Y. M.; Nizalapur, S.; Sankaranarayanan, M.; Sekhar, K. V. G. C. Inhibitors of pantothenate synthetase of Mycobacterium tuberculosis–a medicinal chemist perspective. *RSC advances* **2020**, *10* (61), 37098-37115.
(23) Vallari, D.; Rock, C. Isolation and characterization of Escherichia coli pantothenate permease (panF) mutants. *Journal of bacteriology* **1985**, *164* (1), 136-142.
(24) Cronan Jr, J.; Littel, K.; Jackowski, S. Genetic and biochemical analyses of pantothenate biosynthesis in Escherichia coli and Salmonella typhimurium. *Journal of Bacteriology* **1982**, *149* (3), 916-922.
(25) Bertani, G. Studies on lysogenesis I: the mode of phage liberation by lysogenic Escherichia coli. *Journal of bacteriology* **1951**, *62* (3), 293-300.
(26) Madigan, M. T.; Martinko, J. M.; Parker, J. *Brock biology of microorganisms*; Prentice hall Upper Saddle River, NJ, 1997.
(27) Leonardi, R.; Jackowski, S. Biosynthesis of pantothenic acid and coenzyme A. *EcoSal plus* **2007**, *2* (2), 10.1128/ecosalplus. 1123.1126. 1123.1124.
(28) Kudo, H.; Ono, S.; Abe, K.; Matsuda, M.; Hasunuma, T.; Nishizawa, T.; Asayama, M.; Nishihara, H.; Chohnan, S. Enhanced supply of acetyl-CoA by exogenous pantothenate kinase promotes synthesis of poly (3-hydroxybutyrate). *Microbial Cell Factories* **2023**, *22* (1), 75.
(29) Leonardi, R.; Zhang, Y.-M.; Rock, C. O.; Jackowski, S. Coenzyme A: back in action. *Progress in lipid research* **2005**, *44* (2-3), 125-153.
(30) Jackowski, S.; Rock, C. Regulation of coenzyme A biosynthesis. *Journal of bacteriology* **1981**, *148* (3), 926-932.
(31) Lehninger, A. L. *Lehninger Principles of Biochemistry: David L. Nelson, Michael M. Cox*; Recording for the Blind & Dyslexic New York, 2004.
(32) Holeček, M. Branched-chain amino acids in health and disease: metabolism, alterations in blood plasma, and as supplements. *Nutrition & metabolism* **2018**, *15* (1), 33.

View Article Online
DOI: 10.1039/D6AN00437G

(33) Reitzer, L. Nitrogen assimilation and global regulation in Escherichia coli. *Annual Reviews in Microbiology* **2003**, *57* (1), 155-176.
(34) Ikeda, T. P.; Shauger, A. E.; Kustu, S. Salmonella typhimuriumApparently perceives external nitrogen limitation as internal glutamine limitation. *Journal of molecular biology* **1996**, *259* (4), 589-607.
(35) Jackowski, S.; Rock, C. Metabolism of 4'-phosphopantetheine in Escherichia coli. *Journal of bacteriology* **1984**, *158* (1), 115-120.
(36) Cronan Jr, J. E. Beta-alanine synthesis in Escherichia coli. *Journal of bacteriology* **1980**, *141* (3), 1291-1297.
(37) Rock, C. O.; Cronan, J. E. Escherichia coli as a model for the regulation of dissociable (type II) fatty acid biosynthesis. *Biochimica et Biophysica Acta (BBA)-Lipids and Lipid Metabolism* **1996**, *1302* (1), 1-16.
(38) Jackowski, S. Biosynthesis of pantothenic acid and coenzyme A. *Escherichia coli and Salmonella typhimurium: cellular and molecular biology* **1996**, 687-694.
(39) Vallari, D.; Jackowski, S. Biosynthesis and degradation both contribute to the regulation of coenzyme A content in Escherichia coli. *Journal of bacteriology* **1988**, *170* (9), 3961-3966.
(40) Imlay, J. A. Cellular defenses against superoxide and hydrogen peroxide. *Annu. Rev. Biochem.* **2008**, *77* (1), 755-776.
(41) Chonoles Imlay, K. R.; Korshunov, S.; Imlay, J. A. Physiological roles and adverse effects of the two cystine importers of Escherichia coli. *Journal of bacteriology* **2015**, *197* (23), 3629-3644.
(42) Wortham, B. W.; Oliveira, M. A.; Patel, C. N. Polyamines in bacteria: pleiotropic effects yet specific mechanisms. *The Genus Yersinia: From Genomics to Function* **2007**, 106-115.
(43) Rieck, J.; Skatchkov, S. N.; Derst, C.; Eaton, M. J.; Veh, R. W. Unique chemistry, intake, and metabolism of polyamines in the central nervous system (CNS) and its body. *Biomolecules* **2022**, *12* (4), 501.
(44) Jozefczuk, S.; Klie, S.; Catchpole, G.; Szymanski, J.; Cuadros-Inostroza, A.; Steinhauser, D.; Selbig, J.; Willmitzer, L. Metabolomic and transcriptomic stress response of Escherichia coli. *Molecular systems biology* **2010**, *6*, 364.
(45) Park, J. O.; Rubin, S. A.; Xu, Y.-F.; Amador-Noguez, D.; Fan, J.; Shlomi, T.; Rabinowitz, J. D. Metabolite concentrations, fluxes and free energies imply efficient enzyme usage. *Nature chemical biology* **2016**, *12* (7), 482-489.
(46) Shi, L.; Tu, B. P. Acetyl-CoA and the regulation of metabolism: mechanisms and consequences. *Current opinion in cell biology* **2015**, *33*, 125-131.
(47) Sharma, L. K.; Leonardi, R.; Lin, W.; Boyd, V. A.; Goktug, A.; Shelat, A. A.; Chen, T.; Jackowski, S.; Rock, C. O. A high-throughput screen reveals new small-molecule activators and inhibitors of pantothenate kinases. *Journal of Medicinal Chemistry* **2015**, *58* (3), 1563-1568.

View Article Online
DOI: 10.1039/D6AN00437G

Data for this article, including processed data, raw data files, sample collection, sample preparation, study design, protocol, study metadata, and method, have been uploaded to the Metabolomics Workbench under datatrack ID 7373. Study ID and DOI will be provided once the Metabolomics Workbench review process is complete and the submission is processed.